Temperature correction of electrical resistivity models in time-laspe ERT experiments: towards the integration of model resolution

Arnaud Watlet[1,2], Laurent Gourdol[1], and Olivier Kaufmann[2]
[1]Luxembourg Institute of Science and Technology, Luxembourg - [2]University of Mons, Belgium

Introduction

Electrical Resistivity Tomography (ERT) monitoring is a powerful tool, offering high-resolution imaging of the subsurface. The strong links between resistivity and water content makes ERT monitoring a powerful tool to observe soil moisture and groundwater dynamics. However, temperature significantly influences resistivity measurements —by up to 2% per °C— posing challenges in distinguishing hydrological signals from thermal effects.

Here, we review existing temperature modelling approaches and correction strategies applied to ERT time-lapse datasets in order to remove the effect of temperature variations on resistivity models. This is a critical component of ensuring that hydrological processes can be properly interpreted on ERT images.

Temperature modelling (TM) approaches

The heat equation describes sbsurface temperature variations, primarily driven by air temperature and dependent on thermal properties of the medium

$$\frac{\partial T}{\partial t} = \alpha \nabla^2 T$$

T: Temperature, *t*: time
α: Thermal diffusivity of the material

1D model based on air temperature

Simple 1D models, like the sinusoidal approximation by Brunet et al. (2010), are widely used in ERT studies to model the propagation of air temperature at depth.

$$T(z,t) = T_{mean} + \frac{A}{2} \cdot e^{-z/d} \cdot \sin\left(\omega t - \frac{z}{d} + \phi\right)$$

$T(z,t)$: Temperature at depth z and time t
T_{mean}: Mean annual surface temperature
A: Amplitude of the surface temperature fluctuation
z: Depth below surface
ω: Angular frequency = $2\pi/P$, with P = period (e.g., 1 year)
d: Thermal damping depth = $\sqrt{\frac{2\alpha}{\omega}}$
α: Thermal diffusivity of the subsurface
Φ: Offset to match with actual air temperature

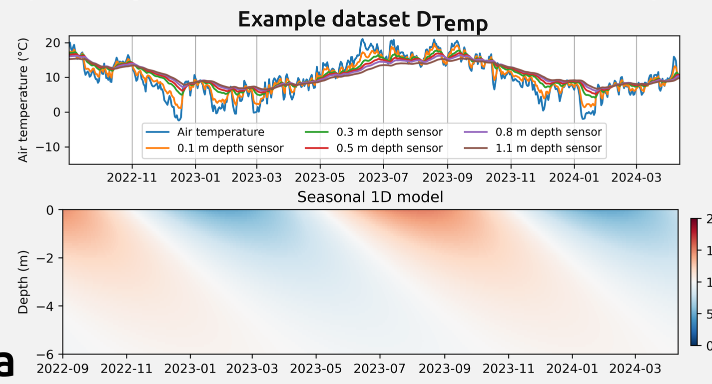

Interpollating temperature data

Interpollating data from a profile of temperature sensors is another approach that has the advantage of reflecting true measurements.

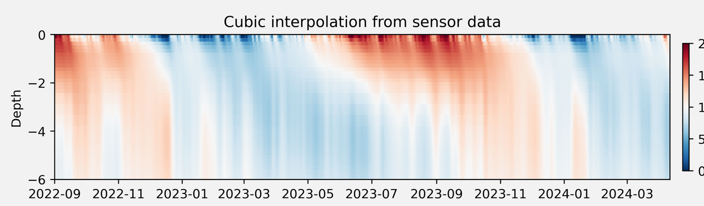

Heat transfer modelling

The finite element modelling solver of pyGIMLI (Rücker et al., 2017) allows to solve the heat equation numerically using the Crank-Nicolson approximation.

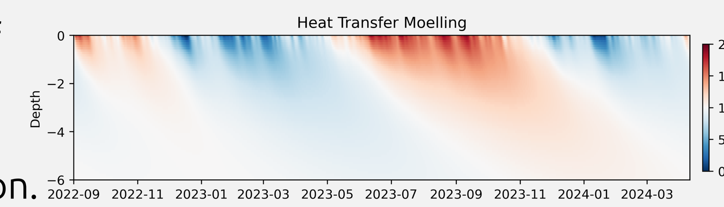

Comparing TM approaches

Choosing the right TM strategy depends on factors such as the ERT time-lapse acquisition frequency and the availability of temperature data at depth.
Sub-daily temperature changes can be difficult to capture with simple 1D models, in which case sensor data interpolation or heat transfer modelling are more appropriate.
For small-scale applications (e.g., monitoring tree stems) or when temperature data is unavailable, heat transfer modelling may be the only viable approach.

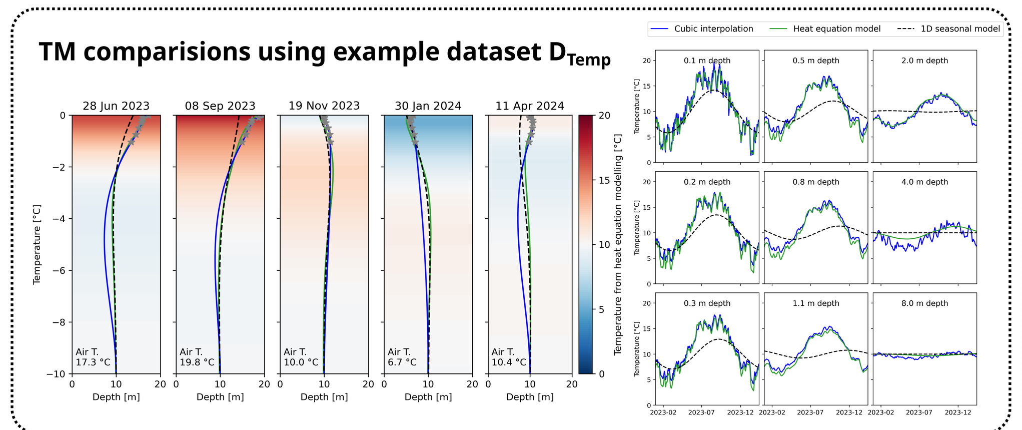

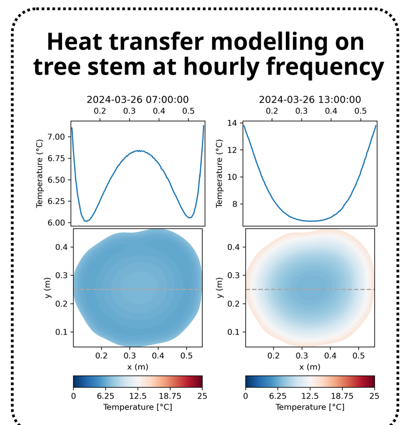

Conversion model

A few conversion models have been proposed to link electrical resistivity and temperature. They are usually based on empirical relaitonships calibrated on samples in the lab. Here, we rely on the KF conversion model proposed by Keller and Frischknecht (1966), defined as:

$$\rho^{TC} = \rho^{T}\,[1 + m_{KF}(T - T_{std})]$$

ρ^{TC}: Resistivity at temperature T_{std}
ρ^{T}: Resistivity at temperature T
T_{std}: Reference temperature (mean annual temperature = 10°C
m_{KF}: Coefficient depending on material type (0.02 to 0.025°C^{-1})

Temperature correction (TC) approaches

Current correction methods rely on simplified temperature models or interpolated sensor data, often neglecting how ERT measurement setups affect sensitivity to temperature. These limitations can introduce artifacts, especially with varied electrode spacing. Here we review existing approaches and propose new strategies.

Simulating temperature effect on synthetic model

We construct a model m_{true} to which a temperature operator T is applied, resulting in m^{T}_{true}. Running forward simulations and inverting the resulting synthetic data gives m_{ref} and m_{est} on which we test 5 TC approaches.

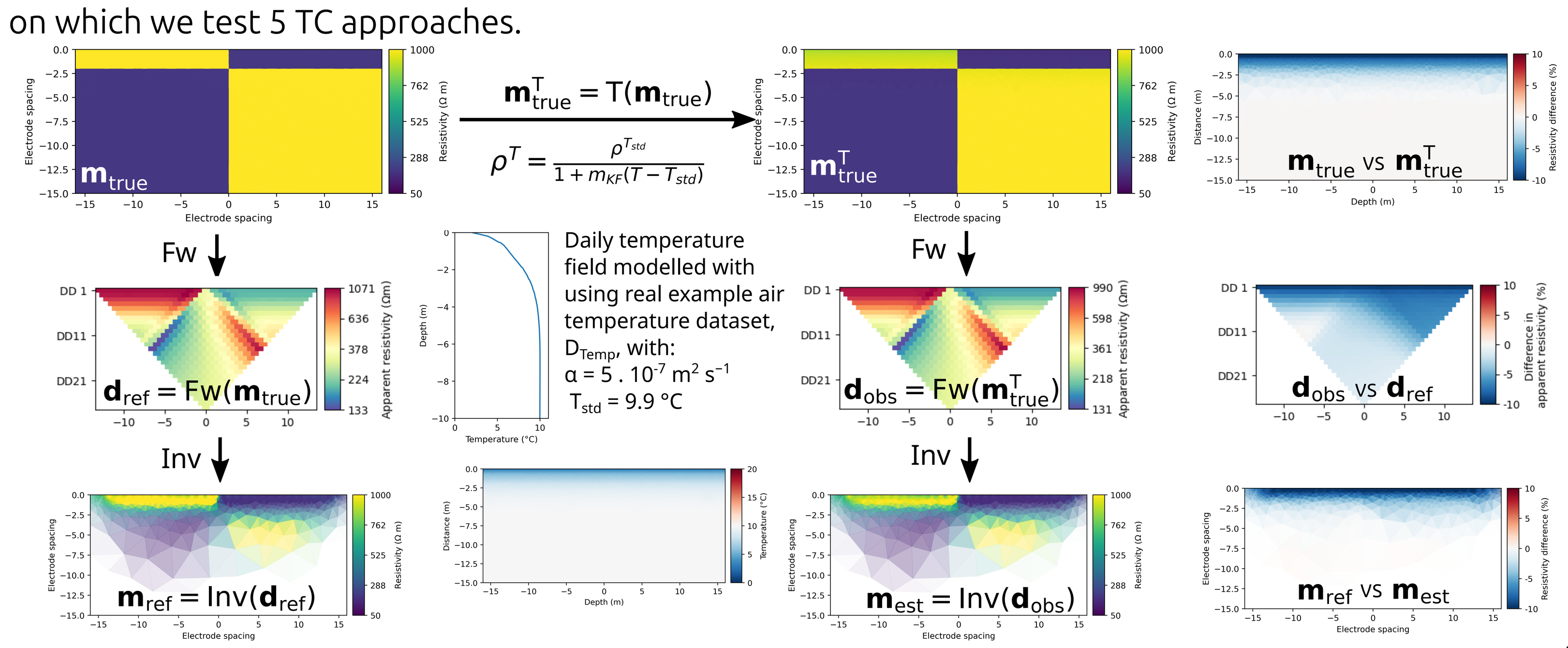

Model-based correction approaches

TC_1 — Conventional model-based correction

Converting each cell's resistivity value to temperature corrected resistivity based on a temperature field mapped on same mesh, and a conversion model (KF).

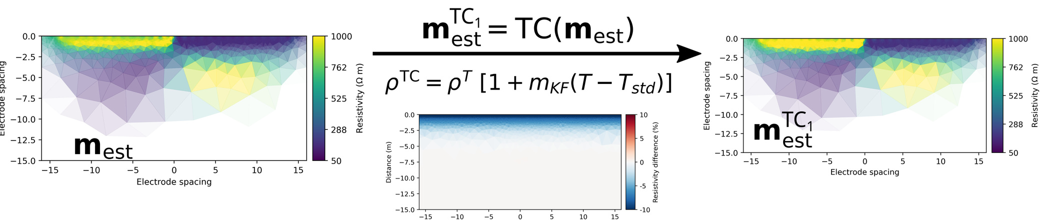

TC_2 — New approach using correction factor deduced from 1-Ω.m model

Applying inverse KF to add the effect of temperature to a 1-Ω.m model (m_{uni})
Deriving correction factor based on forward simulation using same quadrupoles as in d_{obs}
Applying CF to inverted resistivity model

$$m^{TC_2}_{est} = m_{est} \cdot \left(\frac{m_{uni,est}}{m^{T}_{uni,est}}\right) = m_{est} \cdot \left(\frac{1}{m^{T}_{uni,est}}\right)^{CF}$$

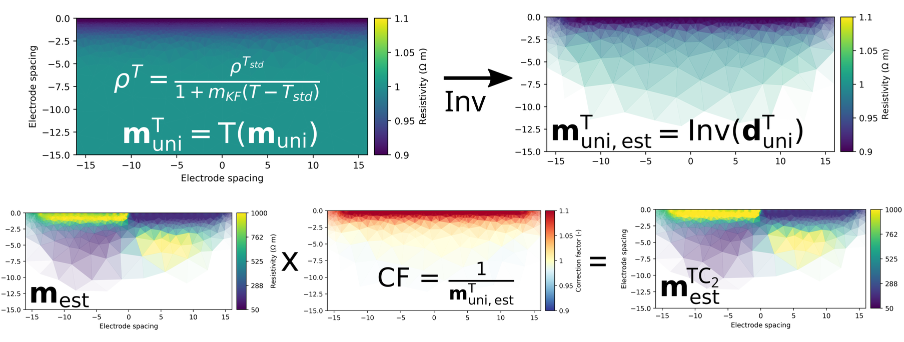

Data-based correction approaches

TC_3 — New approach using correction factor deduced from 1-Ohm.m

A correction factor CF is calculated directly on the apparent resistivities of the model response of the 1-Ohm.m model.

$$d^{TC}_{obs} = d_{obs} \cdot \frac{d_{uni}}{d^{T}_{uni}} = d_{obs} \cdot \left(\frac{1}{d^{T}_{uni}}\right)^{CF}$$

$$m^{TC_3}_{est} = Inv(d^{TC_3}_{obs})$$

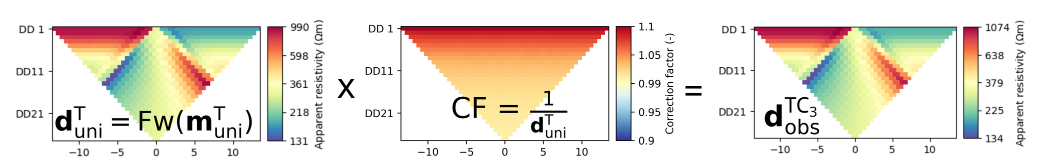

TC_4 — Post-inversion additive CF on model response based on TC_1 (Hayley et al., 2010)

After inverting a first time d_{obs}, an additive CF is calculated based on the difference between the model responses of m_{est} and of $m^{TC,m_{conv}}_{est}$

$$d^{TC_1}_{est} = Fw(m^{TC_1}_{est}) \qquad d_{est} = Fw(m_{est})$$

$$d^{TC_4}_{obs} = d_{obs} + \left(d^{TC_1}_{est} - d_{est}\right)$$

$$m^{TC_4}_{est} = Inv(d^{TC_4}_{obs})$$

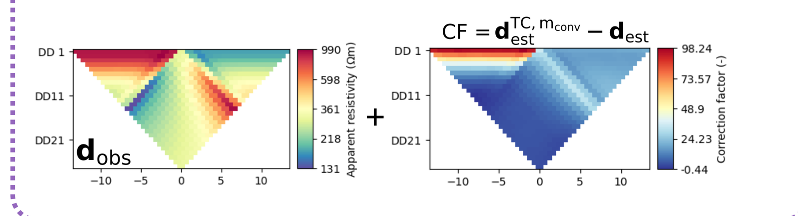

TC_5 — Post-inversion multiplicative CF on model response based on 1-Ω.m model of TC_2

After inverting a first time d_{obs}, a multiplicative CF is calculated based on the ratio between the model responses of m_{est} and of $m^{TC,m_{uni}}_{est}$

$$d^{TC_2}_{est} = Fw(m^{TC_2}_{est}) \qquad d_{est} = Fw(m_{est})$$

$$d^{TC_5}_{obs} = d_{obs} \cdot \left(\frac{d^{TC_2}_{est}}{d_{est}}\right)$$

$$m^{TC_5}_{est} = Inv(d^{TC_5}_{obs})$$

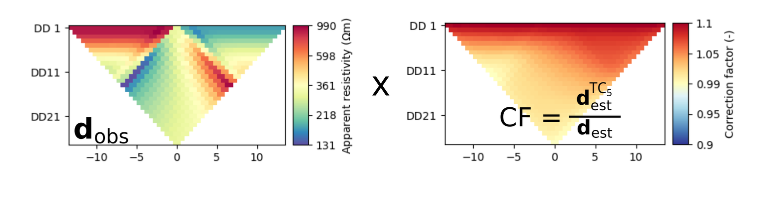

Comparing TC approaches

The 5 TC approaches are tested on varying electrode spacings (from 0.25 m to 10 m) and across the daily air temperature dataset D_{Temp} (at weekly intervals) in order to cover a broad range of subsurface temperature conditions.

Each TC model is compared to the reference model m_{ref}

Spatial distributions of the resistivity differences and the root mean square deviations (RMSD) from m_{ref} are used to characterise the performance of each TC strategy.

TC_1 favours shallow correction artefacts, while TC_3 and TC_4 favour the occurrence of deeper artefacts.

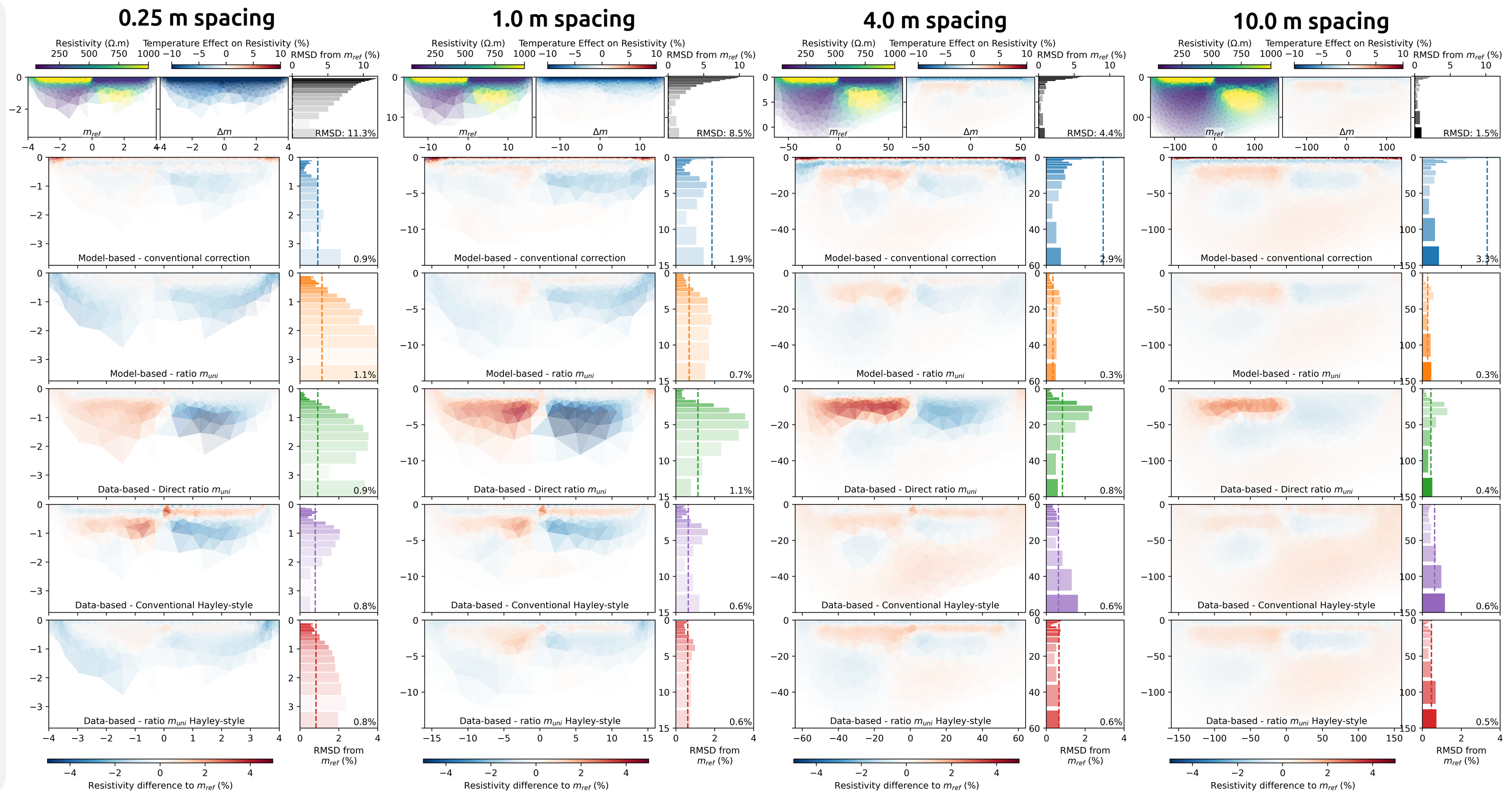

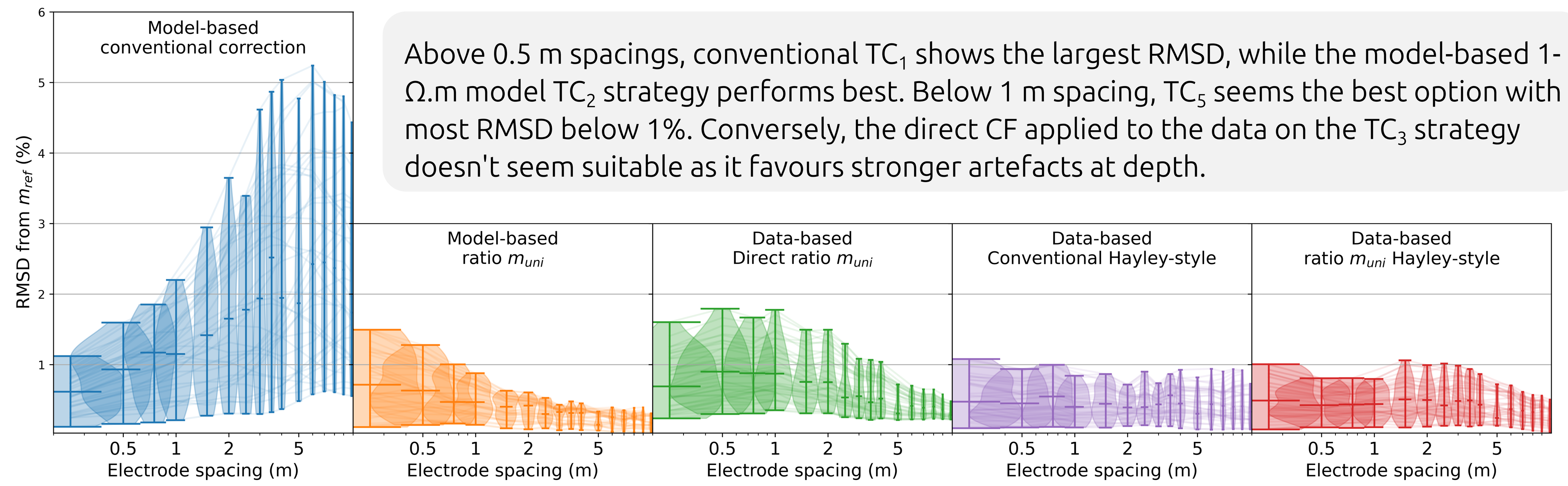

Above 0.5 m spacings, conventional TC_1 shows the largest RMSD, while the model-based 1-Ω.m model TC_2 strategy performs best. Below 1 m spacing, TC_5 seems the best option with most RMSD below 1%. Conversely, the direct CF applied to the data on the TC_3 strategy doesn't seem suitable as it favours stronger artefacts at depth.

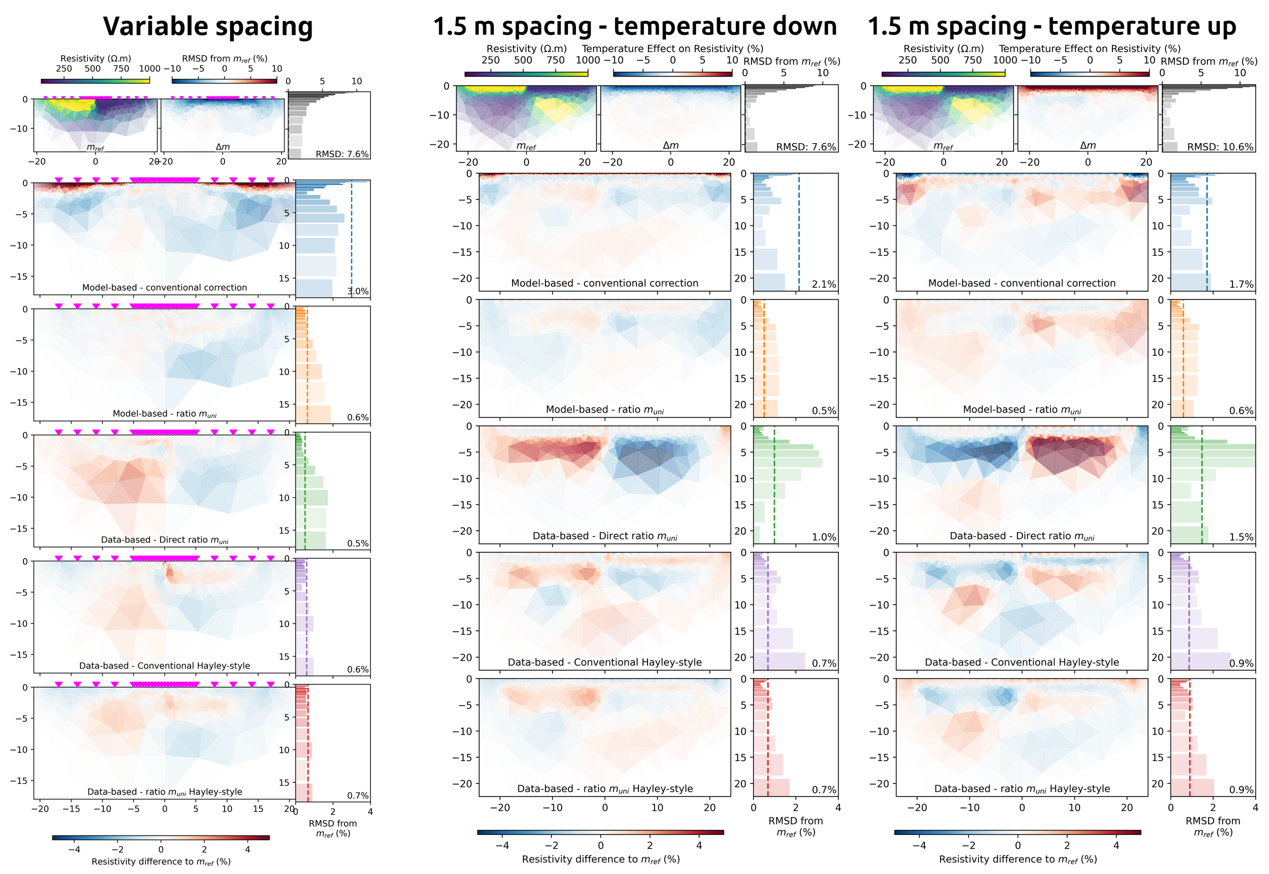

Why does it matter?

Due to the integrative spatial sensitivity of ERT measurements, and spatial constraints in the modelling process shallow temperature variations impacts resistivity models even at depth.

Optimising the TC of time-lapse ERT dataset is critical in order to better extract the signature of hydrological processes.

Chosing sub-optimal TC strategies, like the conventional TC_1 approach can lead to under- or over-corrected resistivity models resulting in biased hydrological interpretations.

Take-home message

Combining heat transfer modelling, to generate high-resolution temperature models, with our newly proposed TC approaches (TC_2 and TC_5) is effective in reducing temperature effects on ERT monitoring datasets.

Additional tests and simulations are required to further validate these strategies, such as with a larger range of thermal properties and ERT acquisition frequency.

References
Brunet, P., Clément, R. and Bouvier, C., 2010. Monitoring soil water content and deficit using Electrical Resistivity Tomography (ERT)–A case study in the Cevennes area, France. Journal of Hydrology, 380(1-2), pp.146-153.
Hayley, K., Bentley, L.R. and Pidlisecky, A., 2010. Compensating for temperature variations in time-lapse electrical resistivity difference imaging. Geophysics, 75(4), pp.WA51-WA59.
Keller, G. V. and Frischknecht, F. C.: Electrical methods in geophysical prospecting, 1966.
Rücker, C., Günther, T., Wagner, F.M., 2017. pyGIMLi: An open-source library for modelling and inversion in geophysics, Computers and Geosciences, 109, 106-123, doi: 10.1016/j.cageo.2017.07.011.